RSC Advances




ROYAL SOCIETY OF CHEMISTRY

www.rsc.org/advances

RSC Advances

PAPER

# Highly responsive glutathione functionalized green AuNP probe for precise colorimetric detection of $Cd^{2+}$ contamination in the environment

Received 00th January 20xx,
Accepted 00th January 20xx

DOI: 10.1039/x0xx00000x

www.rsc.org/

Rajarathinam Manjumeena,*[a] Dhanapal Duraibabu[b], Thangavelu Rajamuthuramalingam[c], Ramasamy Venkatesan[d] and Puthupalayam Thangavelu Kalaichelvan[a]

AuNPs phytosynthesized using the aqueous leaves extract of Rosa indica- wichuriana hybrid Francois guillot showed a well-defined surface plasmon band centered at around 520 nm which is the characteristic of gold nanoparticles. HRTEM micrograph showed that the size of the AuNPs were in the range of 5-13 nm. The AuNPs were functionalized using glutathione via the thiol group from the cysteine moiety to develop highly responsive GSH- AuNPs probe for precise colorimetric detection of $Cd^{2+}$. The functionalization was confirmed by FT-IR. Atomic absorption spectroscopy was used to quantify the heavy metals present in the two water samples collected from the water bodies in Ranipet, a suburb town and industrial hub of Vellore city in the state of Tamil Nadu in southern India. The colorimetric selectivity of the GSH-AuNPs probe to the quantified metal ions $Mg^{2+}$, $Ca^{2+}$,$Ba^{2+}$, $Ni^{2+}$, $Mn^{2+}$, $Cu^{2+}$, $Hg^{2+}$, $Co^{2+}$, $Cd^{2+}$, $Cr^{3+}$, $Fe^{2+}$ was ascertained by UV-Vis spectroscopy. The observations demonstrate that only $Cd^{2+}$ stimulated the GSH- AuNPs solution to turn purple from ruby red and a substantial shift in the SP band to longer wavelength of 594 nm owing to GSH- AuNPs aggregation. The minimum and maximum detection limit of $Cd^{2+}$ by GSH- AuNPs probe was inferred to be 30 nM-70 nM ($3 \times 10^{-8}$ M and $7 \times 10^{-8}$ M) respectively. The feasibility of employing the probe practically in the environment to detect $Cd^{2+}$ was demonstrated using two water samples. The aggregation-based change in color from ruby red to purple resulted in less than 10 min. This result could be considered a straight forward and instantaneous detection of $Cd^{2+}$devoid of any interference from other metal ions those were present in the water samples.

## 1. Introduction

Contamination of the environment with heavy metal ions like Mercury (Hg), lead (Pb), and cadmium (Cd) has been a major concern throughout the world for several decades, as it can cause long-term damage to many biological systems, which can disrupt biological events at the cellular level, and significant oxidative damage as they are also carcinogens. Heavy metal ions can cause severe risk to human health and the environment, it is imperative to develop methods for detecting them at low concentrations that are normally found in environmental samples[1,2]. Even trace amounts of heavy metal ions can pose detrimental risks to human health, so the sensitive, diligent, simple and reliable analysis of heavy metal ions is inevitable[3].

Chemical pollution in water is one of the major threats to the environment, since polluted water poses a negative feedback to human health and welfare, and hinders the sustainable development of both society and the economy. The presence of chemical toxins, heavy metals, inorganic and organic pollutants in water, due to either natural or artificial processes, needs to be monitored constantly to safe guard the supply of clean drinking water to the public, and to control its impact on the environment and the ecosystem[4,5]. Several methods such as electrochemical analysis[6], atomic absorption spectrometry[7,8], inductively coupled plasma atomic emission spectrometry[9] inductively coupled plasma mass spectrometry [10] and molecular fluorescence spectroscopy[11] have been developed for the detection of heavy metals in environmental samples. Most of the methods are expensive, intricate and arduous for in situ detection. In recent years, the combination of nanotechnology, chemistry, physics and biology has enabled the development of ultra-sensitive detection and imaging methods, including applications in electronic, magnetic, environmental, pharmaceutical, cosmetic, energy, opto-electronic, catalytic, and material fields[12,13].

Cadmium is a heavy metal that is released both from natural sources (leaching of cadmium rich soils) and anthropogenic activities (mining, smelting, electroplating, manufacturing of batteries and pigments that utilize cadmium)

[a] CAS in Botany, University of Madras, Guindy Campus, Chennai- 600 025, Tamil Nadu, India.
[b] Department of Chemistry, Anna University, Chennai- 600 025, Tamil Nadu, India
[c] Department of Biotechnology, University of Madras, Guindy Campus, 600 025, Tamil Nadu, India
[d] National Institute of Ocean Technology, Chennai- 600100, Tamil Nadu, India
† Footnotes relating to the title and/or authors should appear here.
Electronic Supplementary Information (ESI) available: [details of any supplementary information available should be included here]. See DOI: 10.1039/x0xx00000x

to the aquatic and terrestrial environments[14]. Moreover, atmospheric deposition of airborne cadmium, and the application of cadmium-containing fertilizers, sewage sludge on farm land may lead to contamination of soils and increased cadmium uptake by crops and vegetables consumed by human beings[15]. Cadmium has been considered more toxic (toxic at levels one tenth) than lead, mercury, aluminium or nickel[16] and ranked the 7th toxicant in the Priority List of hazardous Substances of the Agency for Toxic Substances and Disease Registry[17,18]. Cadmium is regularly found in ores together with zinc, copper and lead. Therefore volcanic activity is one natural reason for a temporary increase in environmental cadmium concentrations. Cadmium is widely used in industrial processes, as an anticorrosive agent, stabilizer in PVC products, color pigment, neutron absorber in nuclear power plants, and in the fabrication of nickel-cadmium batteries. Phosphate fertilizers also show a big cadmium load. Although some cadmium-containing products can be recycled, a large share of the general cadmium pollution is caused by dumping and incinerating cadmium-polluted waste[19]. Cadmium is classified as a prevalent toxic element with biological half-life in the range of 10–30 years, and is known to damage organs such as kidneys, liver and lungs, even at its very low concentration level[20].

For the past decade, nanoparticles (NPs) are being utilized as functional probes for analysing toxins, metal ions, and inorganic and organic pollutants[21] in the field of environmental monitoring. The major hazardous metals of concern for India in terms of their environmental load and toxic effects to human health are lead, chromium, mercury, cadmium, copper and aluminium[22]. Sensing approaches based on NPs aggregation (colorimetric assays) have received considerable attention not only because of their excellent analytical performance exhibited in terms of high selectivity, rapidity, sensitivity, ease of detection but also because of their extreme simplicity and low cost when compared to highly sophisticated instrumental based sensing approaches that are not cost effective, since NPs based colorimetric assays do not require any expensive or complex instrumentation[23].

In recent years, gold nanoparticles (AuNPs) have been widely used as colorimetric probes for chemical sensing and biosensing of various substances[24], such as viruses[25], protein [26], DNA[27], cancerous cells[28], metal ions[29-31] and small molecules [32,33] relying on their unique size-dependent and/or interparticle-distance dependent absorption spectra and solution color. One of the most important characteristics of AuNPs (metal NPs) is their localized surface plasmon resonance (LSPR) which refers to the collective oscillation of the conducting electrons of AuNPs when their frequency matches that of the incident electromagnetic radiation[34]. Strong absorption bands or increased scattering intensity of the radiation occurs at certain wavelengths for the AuNPs as a result of this phenomenon[35]. LSPR of the AuNPs is mainly related to the size, shape, composition, interparticle distance, and dielectric constant (refractive index) of the surrounding medium[36-38]. Based on these exhibiting LSPR features, one of the most interesting fields of work in analytical nanotechnology is related to sensing approaches based on metal NPs aggregation[39]. As gold nanoparticles (AuNPs) have emerged as a promising colorimetric probe that supports naked-eye-based readout methods, even at nanomolar concentrations that show observable red-to-blue color change upon nanoparticle aggregation due to their high extinction coefficient[40-42] there is a need for "green chemistry" that includes a clean, nontoxic, and environment-friendly method of gold nanoparticles synthesis. There are many reports on using chemically synthesized AuNPs as colorimetric sensors for heavy metal detection, some of which are listed in synoptic Table S1[43-61]. From the synoptic table it is worth mentioning that there are not many reports on using AuNPs synthesized using plant extract as colorimetric sensor for heavy metal detection.

As an alternative to conventional physical and chemical methods, biological methods are considered safe and ecologically sound for the nanomaterials fabrication[62,63]. With the development of new protocols based on chemical or physical methods, there is an alarming concern about environmental contamination as the chemical procedures involved in the synthesis of nanomaterials generate a large amount of hazardous by-products. The physicochemical characteristics of the surfaces of AuNPs determine their analytical applications as the sensitivity and the selectivity of these materials are directly related to their surface. In this regard, surface functionalization plays a crucial role in increasing the analytical applicability of AuNPs. Appropriate functionalization of AuNPs can improve their properties and increase their selectivity, consequently enlarging their applications[64]. The high inclination of thiol-containing glutathione (GSH) to bind the surface of AuNPs and the presence of six potential coordination sites for metal binding, intrigued us to exploit those properties and utilize GSH to functionalize the phytosynthesized AuNPs. GSH has two free -COOH groups and a $NH_2$ group to provide a hydrophilic interface and a handle for further reactivity with other functional molecules. GSH plays an important role in heavy metal detoxification in cells in plants, yeasts, and bacteria, allowing the latter to grow in toxic soils. The physiological mechanism of detoxification involves the binding of heavy metal ion clusters by GSH, followed by metal-GSH complex polymerization to form metal sulphide - phytochelatin core-shell nanoparticles[65]. The cysteine residue on GSH renders it an important antioxidant capacity that acts as a substrate for the regeneration of other essential antioxidants[66].

Ranipet is an industrial area located at about 120 km from Chennai on Chennai-Bangalore highway and is a chronic polluted area identified by Central Pollution Control Board of India. It is one of the biggest exporting centers of tanned leather in India. The total number of industries located in and around Ranipet town are 240 tanneries along with ceramic, refractory, boiler auxiliaries' plant, and chromium chemicals. The water bodies in the area are highly contaminated due to industrial effluents showing very high concentrations of toxic heavy metals like cadmium, chromium, copper, nickel, lead and mercury. The concentration levels of these metals are



 

much above the permissible limits in surface water and are health hazards especially for the people working in the tannery industries. It was observed that the people in the area are seriously affected and suffering from occupational diseases such as asthma, chronic ulcers and skin diseases[67]. This explains the reason why water samples were collected from this area for real time demonstration of the GSH- AuNPs colorimetric sensor in the detection of $Cd^{2+}$.

The prominence of the present work stems from the fact that an eco-friendly colorimetric probe with high responsiveness, considerably low detection limit range, and rapid detection time has been devised using GSH functionalized phytosynthesized AuNPs and has also been demonstrated with experimental evidence. To the best of our knowledge, this is the first report on using AuNPs synthesized using the leaves extract of *Rosa indica- wichuriana* hybrid *Francois guillot* in AuNPs- based assays for $Cd^{2+}$. Besides, the present approach has been successfully applied to assess its feasibility to detect $Cd^{2+}$ in heavy metals contaminated water samples.

## 2. Experimental

### 2.1 MATERIALS

Chloroauric acid ($HAuCl_4 \bullet 3H_2O$), trisodium citrate dihydrate, ($Na_3C_6H_5O_7.2H_2O$) glutathione reduced ($C_{10}H_{17}N_3O_6S$) were procured from SRL, Mumbai, India and were used as received without further treatment or purifications. Stock and other aqueous solutions were prepared using Millipore purified water having 18.2 MΩ cm electrical resistivity to rule out any possible interference to the analytical probe. All glassware were thoroughly cleaned with freshly prepared aqua regia (3:1 (v/v) $HCl/HNO_3$ and rinsed thoroughly with Mill-Q (18.2 MΩ cm) water prior to use. The metal salts cadmium chloride ($CdCl_2$), calcium chloride ($CaCl_2$), manganese chloride ($MnCl_2$), magnesium chloride ($MgCl_2$), barium chloride ($BaCl_2$), mercuric chloride ($HgCl_2$), chromium trichloride ($CrCl_3$), ferrous chloride ($FeCl_2$), copper sulphate pentahydrate ($CuSO_4 \bullet 5H_2O$), nickel chloride ($NiCl_2$), cobalt chloride ($CoCl_2$) procured from Sigma-Aldrich, Bangalore, India were used as received to test the selective colorimetric sensitivity of the AuNPs probe to the metal ions $Cd^{2+}$, $Ca^{2+}$, $Mn^{2+}$, $Mg^{2+}$, $Ba^{2+}$, $Hg^{2+}$, $Cr^{3+}$, $Fe^{2+}$, $Cu^{2+}$, $Ni^{2+}$, $Co^{2+}$ respectively.

### 2.2 Collection of heavy metals contaminated water samples

Two samples (sample 1 and sample 2) of heavy metals contaminated water were collected from the water bodies in the industrial and (Fig. S1a) residential area (Fig. S1b) taken for study. These samples were collected in 1-1 capacity, double cap polythene bottles which were thoroughly washed with 1 mol/L nitric acid and left for 2 days in the laboratory followed by thorough rinsing with distilled water to avoid any possible contamination in bottling and every other precautionary measure was taken before filling the bottle with the sample.

### 2.3 Preparation of leaf extract

Aqueous extract of *Rosa indica- wichuriana* hybrid *Francois guillot* was prepared following the procedure as reported in our previous work[68].

### 2.4 Phytosynthesis of gold nanoparticles, characterization and chemical synthesis of gold nanoparticles(control)

For the phytosynthesis of gold nanoparticles, 1 mL of 1 mM $HAuCl_4$ was added to 9 mL of the aqueous extract of *Rosa indica- wichuriana* hybrid *Francois guillot* leaves (Fig. 1a). The overall optimized reaction condition was observed in 1 mM $HAuCl_4$ solution and neutral pH. This setup was incubated in dark at 37˚C under static condition. The solution turned ruby red in color within 20 min (Fig. 1b) indicating the synthesis of AuNPs. After the synthesis process was completed by reducing metal ion solution with leaves extract, surface plasmon resonance of gold nanoparticles was easily confirmed by UV–vis spectroscopy. The reaction mixture was sampled at regular intervals and the absorption maxima were scanned at the wavelength of 400 nm– 800 nm in UNICAM UV 300 spectrophotometer. The phytosynthesized AuNPs gave sharp peak in the visible region of the electromagnetic spectrum. The X-ray powder diffraction data was acquired by PAN analytical X'Pert PRO diffractometer in Bragg–Brentano geometry using step scan technique and Johansson monochromator to produce pure Cu Kα1 radiation (1.5406 Å; 45 kV, 30 mA) in the range of 20°–90°. The peaks were matched with (JCPDS No. 01-1174). The obtained pattern was for fcc cubic crystal structure. The peak plane matched with the card. The crystalline size was calculated from the full-width at half-maximum (FWHM) of the diffraction peaks using the Debye–Sherrer formula (1)

$$D = 0.89 \lambda / \beta \cos \theta \qquad (1)$$

Where, D is the mean grain size, λ is the X-ray wavelength for Cu target, β is the FWHM of diffraction peak and θ is the diffraction angle. In order to measure the size of nanoparticles accurately each peak is Gaussian fitted and also the instrumental broadening is subtracted using Si standard sample broadening. The FT-IR spectra for phytosynthesized AuNPs, were recorded on an IR Affinity-1 SHIMADZU spectrophotometer in transmittance mode in the range of 400 $cm^{-1}$ - 4000 $cm^{-1}$ at a resolution of 4 $cm^{-1}$. For high resolution transmission electron microscope (HRTEM) measurements, a drop of solution containing synthesized gold nanoparticles was placed on the carbon coated grids and kept under vacuum desiccation over night before loading them onto a specimen holder. HRTEM micrographs were taken by

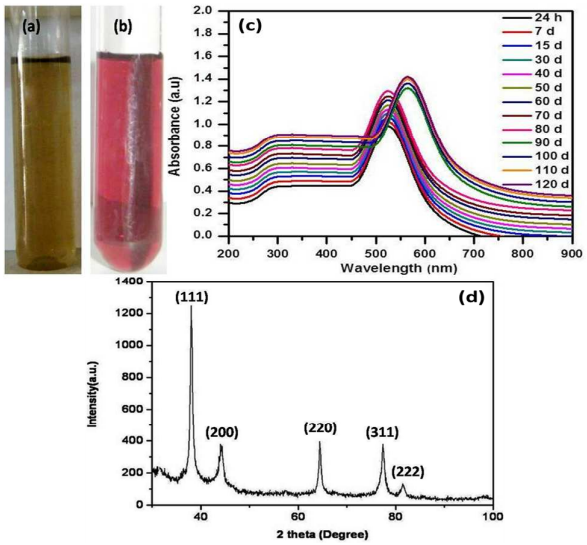


Fig. 1 (a) Aqueous extract of *Rosa indica - wichuriana* hybrid *Francois guillot* (b) Phytosynthesized AuNps (c) UV- Vis spectra of phytosynthesized AuNps at different time intervals (d) XRD pattern of the phytosynthesized AuNPs.

analysing the prepared grids on 300 kv field emission HRTEM FEI, TECHNAI G2 30 S-twin D905 with a capability of energy-dispersive analysis of X-ray (EDAX) attachment. Gold nanoparticles were chemically synthesized using the chemical reduction method as reported by Turkevich et al [69]. To the rapidly-stirred boiling solution of 20 mL of 1 mM tetra chloroauric acid, 2 mL of 1% solution of trisodium citrate dihydrate was added under constant stirring. The gold nanoparticles gradually formed as the citrate reduces the gold. The solution was removed from heat when the solution turned deep red after 10 min.

## 2.5 Optimized preparation of GSH functionalized –AuNPs probes

The Glutathione is a natural tripeptide (GSH) that contains a $NH_2$ group, an –SH and two free -COOH groups to provide a hydrophilic interface and a handle for further reactivity of AuNPs with other functional molecules. GSH was immobilized on the surface of AuNPs via the thiol group from the cysteine moiety. For the optimization and preparation of GSH functionalized-AuNPs probes with designate ratios, in a typical experiment, 300 µL of phytosynthesized AuNPs solution was each added with 0.1 M (pH.8) GSH stock solution of 10 µL, 20 µL, 30 µL, 40 µL, 50 µL, 60 µL, and 70 µL. After being stirred for 90 min at room temperature, each solution was stored at 4°C for at least 48h to ensure self-assembly of the GSH onto the surface of AuNPs before characterization by UV-visible spectroscopy. From the resultant solutions, 0.1 M of 50 µL GSH stock solution added with 300 µL of AuNPs solution was very stable without any observable colour change which is indicative of non-aggregation of AuNPs. Further, the aforementioned stable GSH-AuNPs was purified twice by centrifugation. In each cycle, the supernatant was decanted without disturbing the precipitate for the removal of unadsorbed free GSH molecules in the solution. The precipitate was collected and redispersed in water to obtain the fourier transform infrared (FT-IR) spectra on IR Affinity-1 SHIMADZU spectrophotometer in transmittance mode in the range of 400 $cm^{-1}$ – 4000 $cm^{-1}$ at a resolution of 4 $cm^{-1}$ for the confirmation of the chemical modifications by analyzing the functional groups those were involved in the functionalization method and for further heavy metal detection assay.[70] Similarly, chemically synthesized AuNPs- GSH probe was prepared following the afore-mentioned procedure.

## 2.6 Quantification of heavy metals present in the collected water samples

The two samples (sample 1 and sample 2) of heavy metals contaminated water collected from the areas of study were subjected to atomic absorption spectroscopy analysis to quantify the number of heavy metals and several commonly existing metal ions present in the samples. For reference solutions, 70 nM stock solutions of the metal salts of commonly existing and previously reported metal ions[67] were prepared by individually weighing out a specific amount of the metal salts, transferring into a 100 mL volumetric flask and dissolving completely by adding deionized water to make ionic solution of each metal. Typically, 5 mL each of sample 1 and 2 were used for the analysis. The purity of the reagents and standards used to calibrate the AAS (Atomic absorption spectroscopy- Perkin elmer, Aanalyst 700) instrument is crucial to the analytical accuracy and precision of the results. Reagent blanks were also used to zero the instrument. Therefore, lab reagent water must be of the highest quality to prevent interferences. The account of metal ions detected quantitatively in the two samples of heavy metals contaminated water is tabulated in Table S2.

## 2.7 Colorimetric selectivity test of GSH-AuNPs probe to different metal ions

Having quantified the metal ions present in the two samples of heavy metals contaminated water by atomic absorption spectroscopy, it is indispensable to ascertain the colorimetric selectivity of the developed GSH- AuNPs probe to the detected metal ions. This step is considered crucial to narrow down to one specific heavy metal ion to which the developed GSH-AuNPs probe is colorimetrically sensitive. To scrutinize the metal ions recognition ability of GSH-AuNPs probe, representative alkaline earth metal ions ($Mg^{2+}$, $Ca^{2+}$,$Ba^{2+}$), and transition-metal ions ($Ni^{2+}$, $Mn^{2+}$, $Cu^{2+}$, $Hg^{2+}$, $Co^{2+}$, $Cd^{2+}$, $Cr^{3+}$, $Fe^{2+}$), 0.5 mL of the previously prepared respective metal salts solution were added in the same concentration (70 nM) individually to the solution of GSH-AuNPs (2 mL), and incubated for 20 min at room temperature.[71] As, only the $Cd^{2+}$ metal ion solution induced the colour of GSH- AuNPs solution

to change from ruby red to blue grey under otherwise the same conditions, this indicates the GSH- AuNPs probe is colorimetrically highly specific to $Cd^{2+}$ ions. Furthermore, chemically synthesized AuNPs- GSH probe was used as control to validate the selectivity of phytosynthesized AuNPs - GSH to $Cd^{2+}$. The colorimetric assay could now be narrowed down only to $Cd^{2+}$ ruling out all the other metal ions those were tested for selectivity. This would help us achieve interference free precise detection of $Cd^{2+}$using GSH- AuNPs probe.

### 2.8 Cadmium detection assay using GSH-AuNPs probes

To deduce the minimum detection limit of $Cd^{2+}$ by GSH-AuNPs probe 0.5 mL of standard cadmium solution of 10 nM ($1 \times 10^{-8}$ M), 20 nM ($2 \times 10^{-8}$ M), 30 nM ($3 \times 10^{-8}$ M), 40 nM ($4 \times 10^{-8}$ M), 50 nM ($5 \times 10^{-8}$ M), 60 nM ($6 \times 10^{-8}$ M), 70 nM ($7 \times 10^{-8}$ M) were added individually to 2 mL of GSH-AuNPs solution (λ max=520 nm). The absorption spectra changes of GSH-AuNPs after the addition of different concentrations of $Cd^{2+}$ were scanned at the wavelength of 400 nm– 800 nm in UNICAM UV 300 spectrophotometer. To confirm the feasibility of employing the GSH-AuNPs probe practically in the environment to detect $Cd^{2+}$, the collected heavy metals contaminated water samples (0.5 mL) were added to 2 mL of the GSH-AuNPs solution to check for the changes in absorption spectra and colour change from ruby red to purple.

## 3. Results and discussion

### 3.1 Characterization of the phytosynthesized AuNPs

The UV-Vis spectra (Fig. 1c) show a well-defined surface plasmon band centered at around 520 nm, which is the characteristic of gold nanoparticles and clearly indicates the formation of gold nanoparticles in solution. It may be due to the excitation of surface plasmon resonance (SPR) effect and reduction of$AuCl_4^-$ ions.

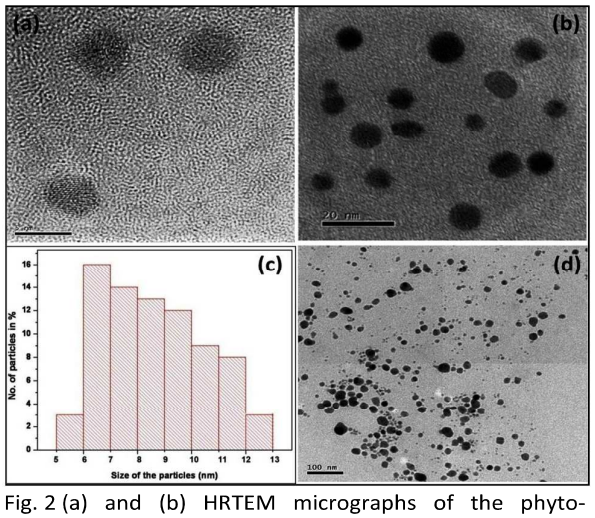


Fig. 2 (a) and (b) HRTEM micrographs of the phyto-synthesized AuNPs (c) Particles size distribution histogram

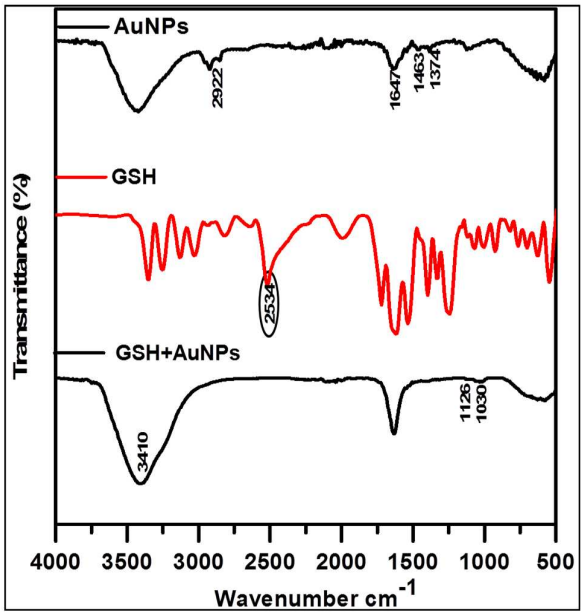


Fig. 3 (a) FT- IR spectrum of AuNPs (b) FT- IR spectrum of GSH (c) FT- IR spectrum of GSH-AuNPs.

The stability results from a potential barrier that develops as a result of the competition between weak Vander Waals forces of attraction and electrostatic repulsion.[72] The solution was stable even after 120 days of synthesis, with no evidence of aggregation of particles. The crystalline nature of AuNPs was confirmed from X-ray diffraction (XRD) analysis. Fig. 1d shows the XRD pattern of the synthesized AuNPs. The five diffraction peaks were observed at 38°, 45°, 67°, 78° and 81° in the 2θ range can be indexed to the (111), (200), (220), (311), (222) reflection planes of face centered cubic structure of metallic gold nanopowders. HRTEM micrographs of the phytosynthesized gold nanoparticles are shown in Fig. 2a and 2b. Monodispersed, discrete spherical shaped gold particle was observed in HRTEM micrograph. HRTEM micrograph showed that the size of the phytosynthesized gold nanoparticles were in the range of 5-13 nm. The particles size distribution histogram determined from micrograph is shown in Fig. 2c. EDAX spectra of gold nanoparticles (Fig. S2) show different X-ray emission peaks with strong signals from the atoms in the gold nanoparticles. This indicates the reduction of gold ions in the chloroauric acid to elemental gold. The average size of the gold nanoparticles was found to be about 12 nm. The FT-IR spectra of AuNPs (Fig. 3a) show the presence of peaks at 2922 $cm^{-1}$, 1647 $cm^{-1}$, 1463 $cm^{-1}$, 1374 $cm^{-1}$. The strong absorption peak at 1647$cm^{-1}$ corresponds to Alkenyl C=C stretch which is the characteristic of gold atoms.[73] The peaks at 2922 $cm^{-1}$, 1463 $cm^{-1}$ and 1374 $cm^{-1}$ correspond to C-H stretching vibration, aromatic ring stretch and methyl C-H symmetrical bend respectively. HRTEM micrograph of chemically synthesized AuNPs (control) showed that the size of the synthesized gold nanoparticles were in the range of 5-20 nm (Fig. S3a and S3b).

### 3.2 Optimized preparation of GSH functionalized–AuNPs probes

AuNPs are very sensitive to change in the concentration of ions in a given solution. Addition of metal salts will alter the ionic balance, screen the electrostatic repulsion between AuNPs and subsequently result in agglomeration. Surface functionalization of such nanoparticles becomes necessary for applications such as colorimetric sensor. The absorption spectra of the nanoparticles after exposure to varying amounts of metal ions are almost identical due to aggregation. It is rather difficult to estimate the concentration of the metal ion to which the AuNPs are precisely sensitive through optical characterization due to the lack of a unique signal for different concentrations. Hence it becomes important to functionalize the AuNps with a material that is not sensitive to the minor changes in electrolyte composition and at the same time exhibits affinity towards the metal ions employed for colorimetric detection[74-77]. The affinity of the GSH towards heavy metals has been well documented in many reports since years. Among the six potential coordination sites for the metal binding, the sulfhydryl site in GSH shows highest affinity towards metal ions like $Cu^{2+}$, $Cd^{2+}$, $Hg^{2+}$ and $Pb^{2+}$ comparing to other sites namely cysteinyl, glutamyl amino, glycyl, glutamyl carboxyl groups and the two peptide linkages[55]. Furthermore, thiol-containing glutathione has high affinity towards the surface of AuNPs that can be finely described by the hard–soft acid-base theory[78]. This explains the reason why GSH was chosen to surface functionalize the phytosynthesized AuNPs. Amongst different range of concentration of 0.1 M GSH from 10 µL upto 70 µL, 50 µL of GSH stock solution added with 300 µL of AuNPs solution was very stable without any observable color change which is indicative of non-aggregation of AuNPs. Fig. 4a shows the UV- Vis absorption spectra of phytosynthesized AuNPs functionalized with 0.1 M GSH from 10 µL upto 70 µL. A hypsochromic shift could be observed in the absorption spectra of 10 µL, 20 µL and 30 µL 0.1 M GSH added to AuNPs. Albeit the stabilization of the AuNPs through a non-covalent interaction with the GSH moiety,10 µL**,** 20 µL and 30 µL were not sufficient enough and directly influences the LSPR of the AuNps in the form of uniform blue shift. Nevertheless, this indicates the specificity of interaction of GSH with AuNps.

The large shifting of the LSPR of AuNPs added with 60 µL and 70 µL 0.1 M GSH might have resulted due to the strong interaction of the thiols with the AuNPs surface, thereby inducing significant charge redistribution, electronic interaction, and forming strong covalent bonds to the surface of AuNPs through back π-bonding from the sulfur[78]. The phytosynthesized AuNPs were found to be quite stable with 50 µL GSH probably due to strong interparticle electrostatic repulsion between the carboxylate anion of glutathione capping on the nanoparticles surface. The stability and non-aggregation of GSH-AuNPs could also be ascribed to the electrostatic repulsion between negatively charged carboxylic groups in the form of zwitterions present in GSH and negatively charged AuNPs. The aforementioned rationale apparently leads to weaker hydrogen bonding interactions and perhaps no aggregation of GSH- AuNPs[79]. Furthermore, the FT- IR spectra of GSH (Fig. 3b) and GSH- AuNPs (Fig. 3c) furnish a strong evidence for the functionalization of AuNps via the thiol group from the cysteine moiety of GSH. The

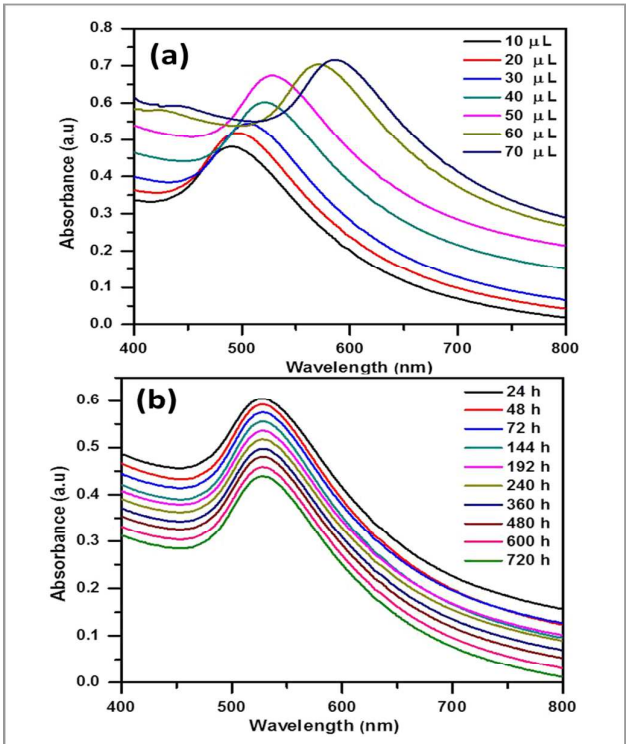


Fig. 4 (a) UV-Vis absorption spectra of AuNps after the addition of different concentration of GSH (b) UV-Vis absorption spectra of AuNPs added with optimized concentration of 50µL GSH at different time interval showing stability.

characteristic absorption peak for–SH at 2534 $cm^{-1}$ which was found in GSH has disappeared in GSH-AuNPs, whereas the peak at 1647 $cm^{-1}$ corresponding to Alkenyl C=C stretch, the characteristic of gold atoms is retained illustrating the stability of AuNPs even after functionalization. HRTEM micrograph of AuNPs functionalized with 50 µL GSH (Fig. 2d) depicts uniform dispersion of GSH-AuNPs

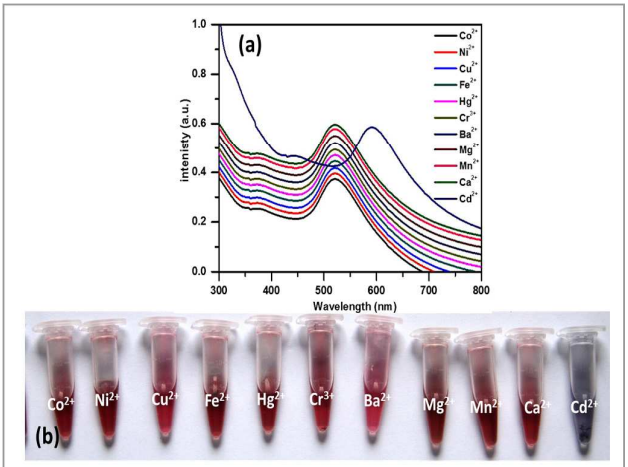


Fig. 5 (a) UV- Vis absorption spectra of GSH-AuNps and (b) the corresponding color change photo images of GSH-AuNps added with different metal ions showing selectivity

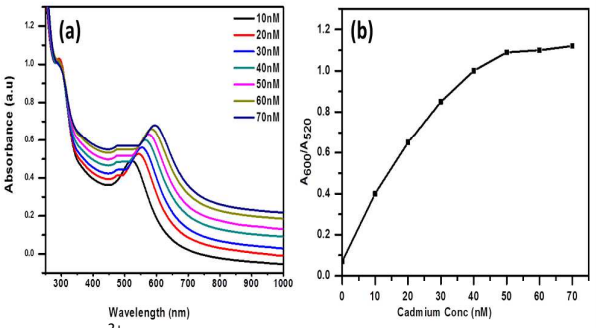


Fig. 6 (a) $Cd^{2+}$ concentration-dependent absorption spectra of GSH-AuNPs (b) Effect of $Cd^{2+}$ concentration on the absorbance ratio of $A_{600}/A_{520}$

with small domains of well-defined and evenly spaced two-dimensional features[80]. This could be attributed to the weak hydrogen bonding of –COOH groups between the adsorbed GSHs and AuNPs leading to the non-aggregated interparticle assembly of GSH- AuNPs. This observation is in concurrence with those reported by H. Li et al. for GSH- AgNPs[71]. The stability of (0.1 M) 50 µL GSH added AuNPs is corroborated by the absorption spectra recorded on different times (Fig. 4b). No obvious change in the shape, position and symmetry of the absorption peak was observed even upto 720 h except for a hypochromic effect towards the end of 720 h. The result indicates GSH-AuNPs are relatively stable over a considerable period of time[71]. Fig. S3c shows the UV-Vis absorption spectra of chemically synthesized AuNps (control) before and after functionalization with GSH.

## 3.3 Colorimetric selectivity test of GSH- AuNPs probe

The colorimetric selectivity test of GSH- AuNPs probe supported by the surface plasmon resonance (SPR) band in Fig. 5a and the corresponding photo images (Fig. 5b) of GSH-AuNPs containing $Mg^{2+}$, $Ca^{2+}$, $Ba^{2+}$, $Ni^{2+}$, $Mn^{2+}$, $Cu^{2+}$, $Hg^{2+}$, $Co^{2+}$, $Cd^{2+}$, $Cr^{3+}$, $Fe^{2+}$ ions (0.5 mL, 70 nM) demonstrate that only $Cd^{2+}$ stimulated the GSH-AuNPs solution to turn purple from ruby red owing to GSH-AuNPs aggregation.

The SPR peak of GSH-AuNPs containing $Cd^{2+}$ ions exhibited broadening and a substantial shift in the plasmon band energy to longer wavelength of 594 nm besides a ruby red-to-purple color change. The mechanism could be attributed to the metal-ligand interaction of $Cd^{2+}$ with GSH in a chelating reaction. The aggregation of GSH-AuNPs could have been induced by the coordination between $Cd^{2+}$ and carboxylate of GSH. $Cd^{2+}$ ion would have formed a complex with GSH via the free sulfhydryl group and also to the carboxyl groups. Similar observation was made by Chai et al., for $Pb^{2+}$ ions[61]. It has been reported that GSH is an efficient detoxification agent of $Cd^{2+}$, which indicates that GSH can strongly interact with $Cd^{2+}$. There are reports that $Cd^{2+}$ could interact with GSH to form a spherical shaped $(GS)_4$ Cd complex while other metal ions, including $Hg^{2+}$ and $Pb^{2+}$, interact with GSH to form linear GS-M-SG complexes. The spherical shaped $(GS)_4$ Cd complex has more net negative charge than that of the linear GS-M-SG, so

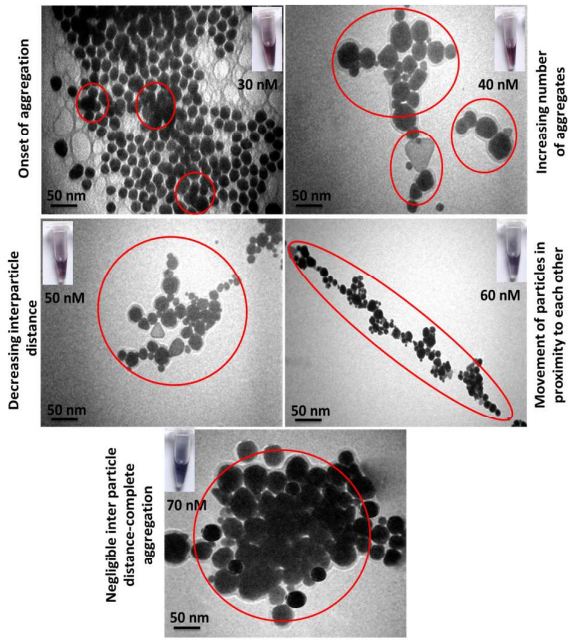


Fig. 7 HRTEM micrographs of GSH-AuNPs added with different concentrations of $Cd^{2+}$ ions and corresponding

the $(GS)_4Cd$ complex shows weaker interaction with AuNPs and cannot stabilize AuNPs well thereby leading to aggregation[43,81]. As H. Li et al., reported that $Ni^{2+}$ ions bind well to groups or ligands containing lone pair electron such as –$NH_2$, –COOH via the coordination bond and as glutathione contains –$NH_2$, and –COOH, both the terminal carboxylate groups of glycine moiety and the free –$NH_2$ groups from glutamate moiety were supposed to be responsible to bind to the Ni(II) center and also participate in cross-linking, we can anticipate the same mechanism to be associated with the $Cd^{2+}$ induced aggregation of GSH - AuNPs and resultant batho-chromic shift as $Cd^{2+}$ belongs to the same group of transition metals as $Ni^{2+}$ [71]. Whereas, the chemically synthesized AuNPs-GSH probe (control) showed colorimetric selectivity to $Cd^{2+}$ besides the interference of $Ni^{2+}$, $Fe^{2+}$, $Hg^{2+}$, $Cr^{3+}$ ions which is depicted in Fig. S4a and S4b as surface plasmon resonance

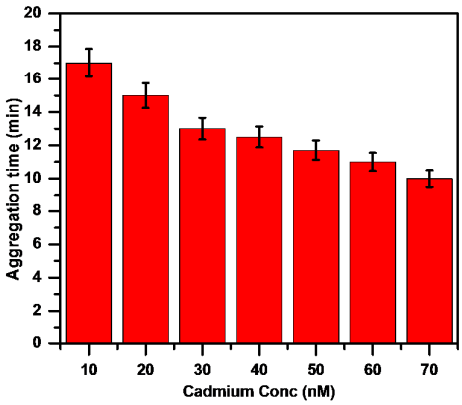


Fig. 8 $Cd^{2+}$ concentration-dependent aggregation time

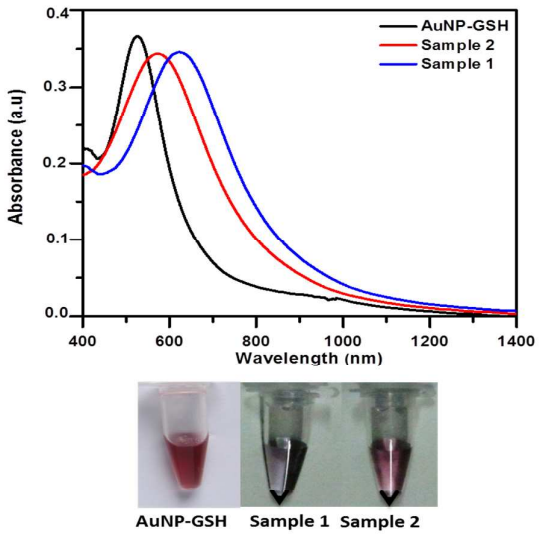


Fig. 9 UV-Vis absorption spectra of GSH-AuNps added with sample 1 and 2 inset-corresponding color change

(SPR) band and the corresponding photo images respectively.

## 3.4 Cadmium detection assay using GSH-AuNPs probes

Fig. 6a illustrates the absorption spectra changes of GSH-AuNPs after the addition of different concentrations of $Cd^{2+}$. The figure manifests that as the concentration of $Cd^{2+}$increases from 10 nM to 70 nM a red shift in wavelength and a broadening of the surface plasmon absorption band occurs accompanying a color change in the solution from ruby red to purple. In the first two cases (10 nM and 20 nM), no spectral and color changes were observed, however upon the addition of 30 nM $Cd^{2+}$ ions a slight bathochromic shift resulted. Apparently, a progressive substantial shift in the plasmon band energy to longer wavelength besides a ruby red-to-purple color change for subsequent concentrations of 40 nM, 50 nM, 60 nM, 70 nM was observed. Therefore, the detection limit depends on the concentration of the metal ions added to the GSH- AuNPs and the minimum and maximum detection limit was inferred to be 30 nM ($3\times10^{-8}$ M) and 70 nM ($7\times10^{-8}$ M)respectively. Fig. 6b shows a linear relation between the ratio of $A_{600}/A_{520}$ and concentration of $Cd^{2+}$ in the range of 10 nM ($1\times10^{-8}$ M) – 70 nM ($7\times10^{-8}$ M). Quite interestingly, the values of absorption ratio $A_{600}/A_{520}$ of GSH-AuNPs were directly proportional to the increase in concentrations of $Cd^{2+}$ ions. This signifies a convincing concurrence to the aforementioned data on the increase in bathochromic shift of the absorption spectra of GSH- AuNPs added with different concentrations of $Cd^{2+}$ ions.

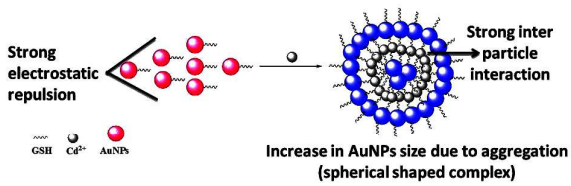


Scheme 1 Hypothetical representation of the mechanism of GSH-AuNPs aggregation after the addition of $Cd^{2+}$

HRTEM micrographs (Fig. 7) of GSH- AuNPs added with different concentrations of $Cd^{2+}$ ions show the increasing order of aggregation of the GSH-AuNPs and subsequent ruby red-to-purple color change (inset). The extent of aggregation depends on the concentration of $Cd^{2+}$ ions in the solution. As the observations indicate plausible red shift of the SP band and the color change from ruby red to purple for the $Cd^{2+}$ concentration of just 70 nM, there is no reason why concentrations beyond 70 nM should be assessed in the detection assay. The aggregation time of GSH-AuNPs added with different concentrations of $Cd^{2+}$ ions are depicted in Fig. 8. The time required for aggregation of GSH- AuNPs is inversely proportional to the concentration of $Cd^{2+}$ ions. This explains that the low concentrations of $Cd^{2+}$ (10 and 20 nM) are too minimum to bring about rapid aggregation of GSH- AuNPs. As the concentration of $Cd^{2+}$increases, the coordination between $Cd^{2+}$ and carboxylate of GSH also increases thereby resulting in complex formation of $Cd^{2+}$with GSH via the free sulfhydryl group and also with the carboxyl groups which can effectively bring AuNPs close to each other. This eventually results in weak electrostatic repulsion and strong electrostatic interparticle interactions between the AuNPs. It has been theoretically proposed and experimentally proven that the plasmon oscillation of metal nanoparticles couple to each other when they are brought in proximity. The close proximity of AuNPs induces coupling of their plasmon oscillation, resulting in a bathochromic shift in the absorption band, reduced zeta potential and consequently aggregation[58]. Since size increases tremendously with aggregation, the LSPR wavelength increases with the increase in particle size due to the near-field coupling in the resonant wavelength peak of the interacting particles[54,82]. The mechanism of GSH-AuNPs aggregation after the addition of $Cd^{2+}$is illustrated graphically in Scheme 1. Fig. 9 shows the absorption spectra of GSH-AuNps which were checked for the feasibility of employing practically in the environment to detect $Cd^{2+}$, it can be seen that the absorbance at 520 nm increased and a new absorption band around 580 nm and 627 nm appeared for sample 2 and 1 respectively which were quantified to contain 25.1 µg/L and 33.6 µg/L of $Cd^{2+}$ respectively from the AAS data. It is worth recalling that the concentration of metal ion is directly proportional to the red shift of the SP band, this would probably justify the reason for the difference in the red shift of the wavelength of GSH-AuNps added with sample 1 and 2 respectively. The aggregation-based change in color from ruby red to purple (Fig. 9 inset) resulted in less than 10 min. This result could be considered a straightforward and instantaneous detection of $Cd^{2+}$devoid of any interference from other metal ions those were present in the water samples as the selectivity of GSH-AuNPs towards other metal ions had been screened experimentally previously.

## 4. Conclusion

A highly responsive GSH functionalized phytosynthesized AuNPs probe for precise colorimetric detection of $Cd^{2+}$ ions was developed and demonstrated taking advantage of localized surface plasmon resonance (LSPR), one of the most important characteristics of AuNPs. The colorimetric selectivity test observations manifest that only $Cd^{2+}$ stimulated the GSH-



 

AuNPs solution to turn purple from ruby red owing to GSH-AuNPs aggregation. The SPR peak of GSH-AuNPs containing $Cd^{2+}$ ions exhibited broadening and a substantial shift in the plasmon band energy to longer wavelength of 594 nm besides a ruby red-to-purple color change due to the metal-ligand interaction of $Cd^{2+}$ with GSH in a chelating reaction and coordination between $Cd^{2+}$ and carboxylate of GSH. The minimum and maximum colorimetric detection limit of $Cd^{2+}$ using GSH-AuNPs probe was inferred to be 30 nM ($3 \times 10^{-8}$ M ) and 70 nM ($7 \times 10^{-8}$ M) respectively. The detection time was 17-11 min. This could be considered a novel contemporary ecofriendly gold nanoparticle based colorimetric nanosensors for cadmium detection in environmental sample among the reports proclaimed so far. The GSH-AuNPs probe was also employed practically to detect $Cd^{2+}$ in heavy metals contaminated water samples. The aggregation-based change in color from ruby red to purple resulted in less than 10 min. Another direction for future research in the present work is, the GSH-AuNps could be rendered luminescence and coated over an appropriate hydrophobic, thermostable substrate to develop colorimetric sensor dip strip. The color change from ruby red to purple could be monitored using UV light. And, perhaps our current efforts are also directed towards improving the colorimetric detection limit. In pursuit of the above mentioned direction more in-depth research is imperative to improve the feasibility, sensitivity and stability of the system towards visual colorimetric detection which are under investigation in our laboratory.

## Acknowledgements

We would like to thank Dr. N. Mathivanan, Director, CAS in Botany, University of Madras, Guindy campus, for providing lab facilities, UGC- BSR for providing a Research fellowship in Sciences and NCNSNT, University of Madras, Guindy campus for providing characterization studies.

## References

1 S. K. Porter, K.G. Scheckel, C. A. Impellitteri and J. A. Ryan, Crit.Rev. Environ. Sci. Technol. **34**, 495 (2004).
2 L. Zhang and M. H. Wong, Environ. Int. **33**, 108 (2007).
3 Y. Kim, R.C. Johnson and J.T. Hupp, Nano Lett. **4**, 165 (2001).
4 G. F. Duan, Z. B. Zhang, J. P.Zhang, Y. J. Zhou, L. Q. Yu and Q. S. Yuan, Crop. Prot, **26**, 1036 (2007).
5 L. Wang, W. Ma, L. Xu, W. Chen, Y. Zhu, C. Xu and N. A. Kotov, Mater. Sci. Eng. R., **R70**, 265 (2010).
6 C.M. Willemse, K. Tlhomelang, N. Jahed, P.G. Baker and E.I. Iwuoha, Sensors. **11**, 3970 (2011).
7 A. Malekpour, S. Hajialigol and M.A. Taher, J. Hazard.Mater. **172**, 229 (2009).
8 M.G.A. Kom, G.L. Dos Santos, S.M. Rosa, L.S.G. Teixeira and P.V. De Oliveira, Microchem. J., **96**, 12 (2010).
9 A. Matsumoto, S. Osaki, T. Kobata, B. Hashimoto, H. Uchihara and T. Nakahara, Microchem. J. **95**, 85 (2010).
10 W. Guo, S. Hu, Y. Xiao, H. Zhang and X. Xie, Chemosphere. **81**, 1463 (2010).
11 S. Yunus, S. Charles, F. Dubios and E. Vander Doncket, J.Fluoresc. **18**, 499 (2008).
12 M. Auffan, J. Rose, J. Y. Bottero, G.V. Lowry, J. P.Jolivet and M. R. Wiesner, Nat.Nanotechnol. **4**, 634 (2009).
13 Z. Wang and L. Ma, Coord. Chem. Rev. **253**, 1607 (2009).
14 S.Chora, M.Starita-Geribaldi, J.M. Guigonis, M.Samson, M.Romeo and M.J.Bebianno, Aquat. Toxicol. **94**, 300 (2009).
15 L.Jarup and A.Akesson, Appl. Pharmacol. **238**, 201 (2009).
16 L. Wilson, Cadmium: The pseudo-masculine mineral and a death mineral, http://www.drlwilson.com/articles/cadmium.htm.
17 ATSDR, The 2007 CERCLA Priority List of Hazardous Substances, Agency for Toxic Substances and Disease Registry. In: U.S. Department of Health and Human Services , Atlanta, GA, 2007.
18 E.R.Siu, D.D.Mruk, C.S.Porto, C.Y.Cheng, Toxicol. Appl. Pharmacol. **238**, 240 (2009).
19 L. Jarup, Br. Med. Bull. **68**, 167 (2003).
20 A.C. Davis, P. Wu, X.F. Zhang, X.D. Hou and B.T. Jones, Appl. Spectrosc. Rev. 41, **35** (2006).
21 J. W. Cheon and J. H. Lee, Acc. Chem. Res., **41**, 1630 (2008).
22 S.K. Sahni, Toxicity and management, Indian National Science Academy position paper, **1**, India, (2011).
23 D.Vilela, M. C. Gonzalez and A.Escarpa, Anal. Chim. Acta. **751**, 24 (2012).
24 W. Zhao, M. A. Brook and Y. F. Li, Chembiochem. **9**, 2363 (2008).
25 K. Niikura, K. Nagakawa, N. Ohtake, T. Suzuki, Y. Matsuo H. Sawa and K. Ijiro, Bioconjugate Chemistry. **20**, 1848 (2009).
26 Y. L. Wang, D. Li, W.Ren, Z. J. Liu, S. J. Dong and E. K. Wang, Chemical Communications. **22**, 2520 (2008).
27 M. Cho, M. S. Han and C. Ban, Chemical Communications. **38**, 4573 (2008).
28 C. D. Medley, J. E. Smith, Z. Tang, Y. Wu, S. Bamrungsap and W. H. Tan, Analytical Chemistry. **80**, 1067 (2008).
29 Y. J.Fan, Z.Liu, L.Wang and J. H. Zhang, Nanoscale Research Letters. **4**, 1230 (2009)
30 J. H.Lee, Z. D.Wang, J. W.Liu and Y. Lu, Journal of the American Chemical Society. **130**, 14217 (2008).
31 X. W.Xu, J.Wang, K. Jiao and X. R. Yang, Biosensors & Bioelectronics. **24**, 3153 (2009).
32 L.Li, and B. X.Li, Analyst. **134**, 1361 (2009).
33 J.Zhang, L. H.Wang, D.Pan, S. S. Pong, F. Y. C.Boey, H.Zhang and C. Fan, Small, **4**, 1196 (2008).
34 A.M. Lopatynskyi, O.G. Lopatynska, L.J. Guo and V.I. Chegel, IEEE Sens. J. **11**, 361 (2011).
35 S.R. Beeram and F.P. Zamborini, J. Phys. Chem. C. **115**, 7364 (2011).
36 K.A. Willets and R.P. Van Duyne, Annu. Rev. Phys. Chem. **58**, 267 (2007).
37 M.E. Stewart, C.R. Anderton, L.B. Thompson, J. Maria, S.K. Gray, J.A. Rogers and R.G. Nuzzo, Chem. Rev., **108**, 494 (2008).
38 Y.H. Ngo, D. Li, G.P. Simon and G. Garnier, Adv. Colloid Interface Sci., **163**, 23 (2011).
39 R. Elghanian, J.J. Storhoff, R.C. Mucic, R.L. Letsinger and C.A. Mirkin, Science. **277**, 1078 (1997).
40 S.I. Stoeva, J.S. Lee, J.E. Smith, S.T. Rosen and C.A. Mirkin, J. Am. Chem. Soc. **128**, 8378 (2006).
41 M.S. Han, A.K.R. Lytton-Jean, B.K. Oh, J. Heo and C.A. Mirkin, Angew. Chem. Int. Ed., **45**, 1807 (2006).
42 J. Li, S.P. Song, X.F. Liu, L.H. Wang, D. Pan, Q. Huang, Y. Zhao and C.H. Fan, Adv. Mater. **20**, 497 (2008).
43 Y. Guo, Y. Zhang, H. Shao, Z. Wang, X.Wang and X. Jiang, Anal. Chem. **86**, 8530 (2014).
44 Y. Xue, H. Zhao, Z. Wu, X. Li, Y. He and Z. Yuan, Analyst. **136**, 3725 (2011).
45 Z.Yuan, M. Peng, Y. He and E.S. Yeung, Chem. Commun. **47**, 11981 (2011).
46 W. Chen, X. Tu and X. Guo, Chem. Commun. 1736 (2009).

47 L. Guo, J. Zhong, J. Wua, F.F. Fu, G. Chen, X. Zheng and S. Lin, Talanta. **82**, 1654 (2010).
48 H. Li, J. Guo, H. Ping, L. Liu, M. Zhang, F. Guan, C. Sun and Q. Zhang, Talanta. **87**, 93 (2011).
49 G. Fu, W. Chen, X. Yue and X. Jiang, Talanta. **103**, 110(2013).
50 Y. Guo, Z. Wang, W. Qu, H. Shao and X. Jiang, Biosensors and Bioelectronics. **26,** 4064 (2011).
51 M. H. Mashhadizadeh, K. Eskandari, A. Foroumadi and A. Shafiee, Electroanalysis. **20**, 1891(2008).
52 C. Radhakumary and K. Sreenivasan, Anal. Chem. **83**, 2829 (2011).
53 I. Y. Kim, R. C. Johnson and J. T. Hupp, Nano Lett. **1**, 165(2001).
54 G. K. Darbha, A. K. Singh, U. S. Rai, E. Yu, H. Yu, and P. C. Ray, J. AM. chem. soc. **130**, 8038(2008).
55 A. Sugunan, C. Thanachayanont, J. Dutta and J.G. Hilborn, Science and Technology of Advanced Materials. **6**, 335(2005).
56 X. Xue, F. Wang, and X. Liu, J. AM. chem. soc. **130**, 3244(2008).
57 D. Maity, A. Kumar, R. Gunupuru and P. Paul, Colloids and surfaces A: Physicochemical and engineering aspects. **455**, 122(2014).
58 K. Yoosaf, B.I. Ipe, C.H. Suresh and K.G. Thomas, J. Phys. Chem. C. **111**, 12839 (2007).
59 C.V. Durgadas, V.N. Lakshmi, C.P. Sharma and K. Sreenivasan, Sensors and Actuators B. **156**, 791(2011).
60 A. Senthamizhan, A. Celebioglu and T. Uyar, J. Mater. Chem. A. **2**, 12717 (2014).
61 F.Chai, C. Wang, T. Wang, L. Li and Z. Su, Applied materials and interaces . **2**, 1466 (2010).
62 S.Shankar, A.Rai, A.Ahmad and M.Sastry, J. Colloid.Interface.Sci. **275**, 496 (2004).
63 N. Kaushik, M.S. Thakkar, S. Snehit, M.S. Mhatre, Y. Rasesh, and M.S. Parikh, Nanomedicine: Nanotechnology, Biology and Medicine, **6**, 257 (2010).
64 S. Thatai, P. Khurana, J. Boken, S. Prasad and D. Kumar, Microchemical Journal. **116**, 62 (2014).
65 E.Grill, E.L.Winnacker and M. H. Zenk, Science, **230**, 674 (1985).
66 K.Smeets, K.Opdenakker, T. Remans, S. Van Sanden, F. Van Belleghem, B.Semane, N.Horemans, Y.Guisez, J.Vangronsveld and A.Cuypers, J. Plant Phys. **166**, 1982 (2009).
67 S. SrinivasaGowd and P.K. Govil, Environ Monit Assess., **136**, 197 (2008).
68 R. Manjumeena, M. Girilal, M. Peter, J. Sudha and P.T. Kalaichelvan, Int. J. Curr.Sci. **8**, 1 (2013).
69. J. Turkevich, P.C. Stevenson and J. Hillier, Discuss. Faraday Soc., **11**, 55 (1951).
70 G. Tan and D. Xiao, J. Hazard. Mater. **164**, 1359 (2009).
71 H. Li, Z. Cui and C. Han, Sensors and Actuators B. **143**, 87 (2009).
72 P. Mulvaney, Langmuir. **12**, 788 (1996).
73 R.Geethalakshmi and D.V.Sarada, Ind. Crop. Prod. **51**, 107 (2013).
74 L. Wang, X. Liu, X. Hu, S, Song and C. Fan,Chem. Commun. **42**, 3780 (2006).
75 H. Wei, B. Li, J. Li, E. Wang and S. Dong, Chem. Commun. **43**, 3735(2007).
76 J. H. Lee, Z. Wang, J. Liu and Y. Lu, J. Am. Chem. Soc., **130**, 14217(2008).
77 N. Ballatori, Adv. Pharmacol. **27**, 271 (1994).
78 S. K. Ghosh, S. Nath, S. Kundu, K. Esumi, and T. Pal, J. Phys. Chem. B. **108**, 13963 (2004).
79 M.R. Hormozi-Nezhada, E. Seyedhosseini and H. Robatjazi, Scientia Iranica. **19**, 958 (2012).
80 I.S. Lim, W. Ip, D. Mott, P.N. Njoki, C.J. Zhong, Y. Pan, S. Zhou and C.J. Zhong, Langmuir. **24**, 8857 (2008).
81 K.L. Pei, M. Sooriyaarachchi, D.A. Sherrell, G.N. George and J. Gailer, J. Inorg. Biochem. **105**, 375 (2011).
82 K.H. Su, Q.H. Wei and X. Zhang, Nano Lett. **3**, 1087 (2003).




 

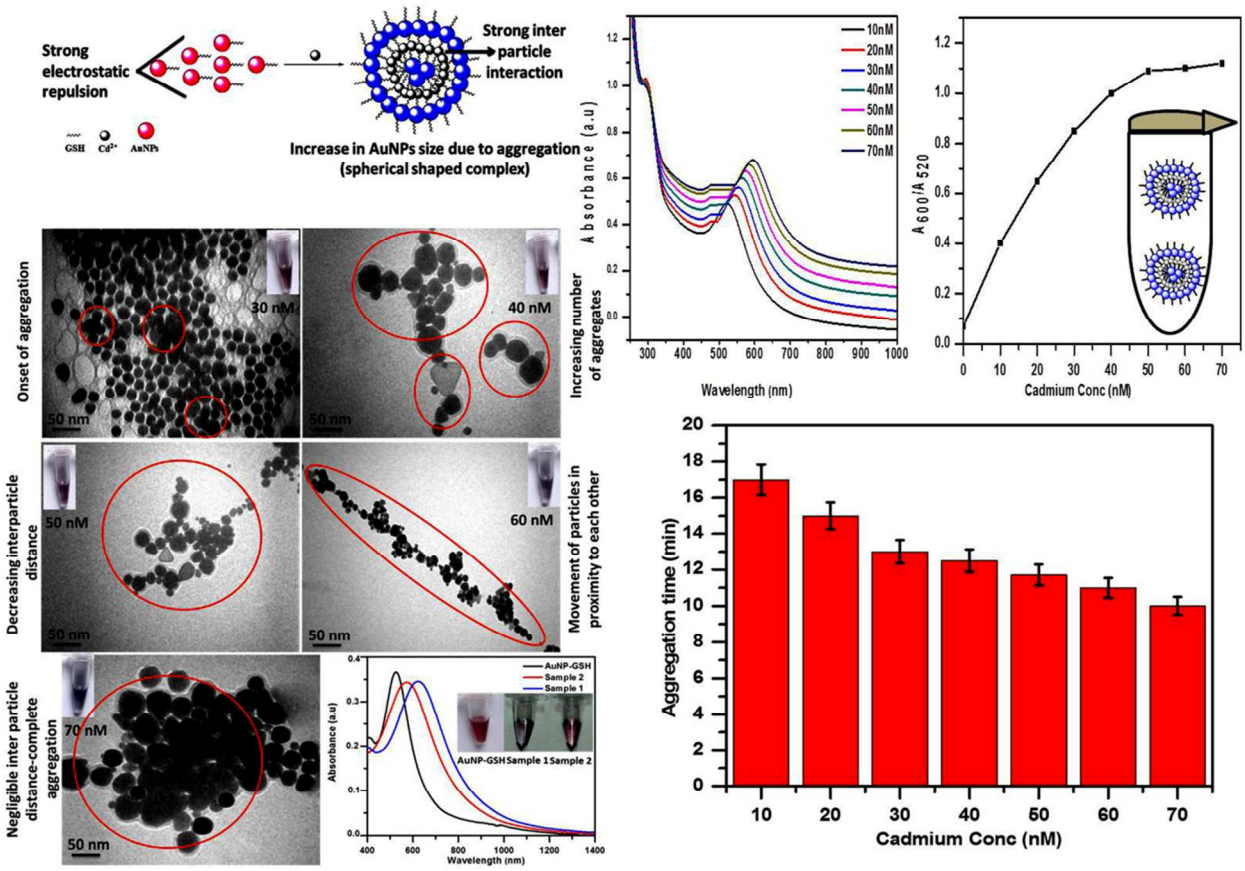


Precise colorimetric detection of $Cd^{2+}$ using glutathione functionalized phytosynthesized AuNP probe- An ecofriendly approach in heavy metal detection